Mining Science, vol. 29, 2022, 19–39

www.miningscience.pwr.edu.pl

Mining Science

(Previously Prace Naukowe Instytutu Gornictwa Politechniki Wroclawskiej, ISSN 0370-0798)

ISSN 2300-9586 (print)
ISSN 2353-5423 (online)

Received April 30, 2021; Reviewed; Accepted July 11, 2022

RESEARCH ON KEY PARAMETERS OF GOB-SIDE ENTRY RETAINING FORMED BY ROOF CUTTING OF WORKING FACE UNDER GOAF IN CLOSE DISTANCE COAL SEAMS

Fuxin SHEN [1,2,3]* ; Yanqi SONG[1,3]; Wenchao ZHAO[2,3]; Hongfa MA[3]; Junjie ZHENG[3]; Zhixin SHAO[3]

[1] State Key Laboratory of Coal Resources and Safe Mining, China University of Mining & Technology (Beijing), Beijing, 100083, China
[2] State Key Laboratory for Geomechanics and Deep Underground Engineering, China University of Mining & Technology (Beijing), Beijing, 100083, China
[3] School of Mechanics and Civil Engineering, China University of Mining & Technology (Beijing), Beijing, 100083, China

Abstract: In order to solve the application problem of gob-side entry retaining formed by roof cutting (GERRC) technology of working face under goaf in close-distance coal seams, the 9101 working face and its return air roadway of Xiashanmao Coal Mine were taken as engineering background. The key parameters of GERRC were studied by means of theoretical analysis, numerical simulation and field test. The results show that: The roof cutting height (RCH) should be not less than the height of stope caving, meanwhile, when the rock strata collapsed, broke and expanded within RCH, it should meet the support effect on basic roof. And the RCH should be less than the distance between coal seams. The roof cutting angle (RCA) should meet the mechanical conditions of rock mass failure along the structural plane, and it should meet the geometric condition of not squeezing the roadway roof during the rotation and subsidence of the stope basic roof. When the RCH was 7.5m, the RCA was 15 degrees and the blasting charge structure was 4+3+3+2, the stress distribution and roof subsidence were most optimal. Three rows of constant resistance with large deformation (CRLD) anchor cables were used to strengthen roadway roof. The unit support, hydraulic prop and π-shaped beam were carried out as temporary support in roadway. The surrounding rock of roadway tended to be stable when lagged behind 100m, and the effect of GERRC was good after the temporary support measures were withdrawn.

Keywords: *Close-distance coal seams; Under goaf; Roof cutting and pressure relief; Roadway formed automatically; Key parameters*

* Corresponding author: sfx803@163.com (F. Shen)
doi: 10.37190/msc222902

1. INTRODUCTION

As one of main energy consumption in China, coal resource has the characteristics of wide distribution and abundant reserves. However, the hosting environment of coal resource is complex, and the problem of close-distance minable coal seams exists in most mining areas. The upper coal seam mining will have disturbance on rock mass and mining in lower coal seam. It belongs to the typical "close-distance" coal seams mining problem (Teng et al (2016); Hao et al (2019)). Many researches have been done on the roadway surrounding rock stability control when mining downward. The theoretical analysis, numerical simulation and laboratory test were used to study the reasonable mining roadway position of the lower coal seam, and the reasonable layout offset of the roadway was obtained (Yan et al. 2015; Gao et al. 2020; Wang et al. 2015; Cheng et al. 2015). Sun et al (2014) studied the failure mode of roof between coal seams, and pointed out that the solid coal side of gob-side entry was mainly cataclastic structure, and the other location was mainly block structure. Wang et al (2018) studied the control technology of mining roadway under the goaf and proposed that increasing the coal pillar size and strengthening support structure can control the surrounding rock deformation. Shi et al (2013) obtained the calculation formula of floor failure depth caused by coal seam mining through field investigation. However, previous research has solved the practical problems of close-distance coal seams mining, and pointed out that coal seam mining will cause damage to floor rock strata, but it cannot fundamentally solve the problems of large roadway excavation and low recovery rate in the process of close-distance coal seam mining.

In order to solve the above problems, He et al (2003) took advantage of the weak tensile strength of rock, and put forward bilateral cumulative tensile explosion (BCTE) technology. Subsequently, the theory of "roof cutting short-wall beam" was proposed. Basing on this theory, a new technology of gob-side entry retaining formed by roof cutting and pressure releasing (GERRC) without coal pillar was developed and applied in the field for the first time successfully (He et al 2015; Zhang et al 2011; Wang et al 2018; Zhang et al 2020). Zhang et al (2020) studied the holes spacing of BCTE, and put forward the spacing calculation formula. In order to cut off the connection between the roadway roof and the stope roof, the key parameters of GERRC are to determine the appropriate roof cutting height (RCH), roof cutting angle (RCA) and roof cutting blasting charge structure, Sun et al (2014) studied the key parameters of thin coal seam, pointed out that the RCA should meet the requirement of the tensile failure of immediate roof and deflect a certain angle towards gob in order to cut off the stress transfer path between the roof of stope and the roof of retaining roadway. Hu et al (2019) proposed a roof-cutting mechanical model of GERRC, determined the optimal RCH, RCA and support measures in a deep inclined thick coal seam. He et al (2018) pointed out the key parameters of roof cutting under deep high stress conditions, and the field support design was optimized. Sun et al(2020) explored the mechanism of GERRC, studied the different modes of collapse between the conventional gob-side entry retaining and GERRC. Guo et al(2019) proposed a novel support system with a good energy-absorbing capacity to make it possible to effectively restrain the large deformation in the deep surrounding rock. However, the above researches were based on single coal seam, the application research of GERRC in close-distance coal seams is less. In order to change the traditional mining mode in close-distance coal seams, expand the application range of GERRC and improve the mining rate, it is necessary to carry out technical research test in the working face under the goaf in close-distance coal seams and study the key parameters of roof cutting. Therefore, the 9101 working face and its return air roadway under goaf in Xiashanmao Coal Mine were taking as engineering background, the reasonable key parameters of roof cutting were studied through theoretical analysis, numerical simulation and field test.

2. ENGINEERING BACKGROUND

Xiashanmao Coal Mine is located in Lvliang City, Shanxi Province, China. The minable coal seams are NO.4, NO.8 and NO.9. The average coal seam spacing between NO.4 and NO.8 is 61.30 m. The average coal seam spacing between NO.8 and NO.9 is 12.20m. The NO.8 coal seam had been fully mined. The technology of GERRC was tested at 9101 working face. The lithology comprehensive column diagram of roof and floor is shown in Fig.1(a).

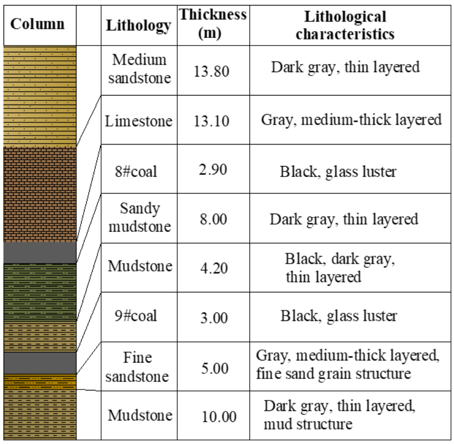

(a)

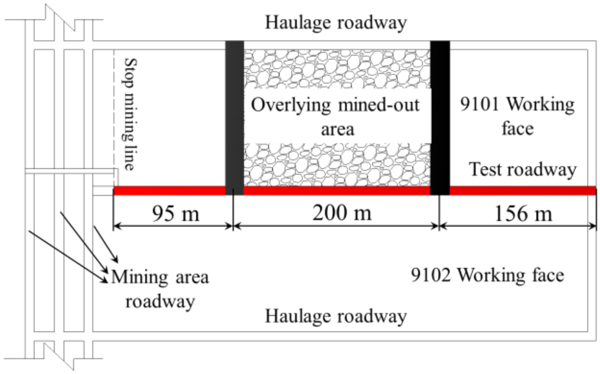

(b)

Fig.1 The lithology histogram and working face layout. (a) Lithology histogram of roof and floor; (b) Layout of working face

At present, NO.9 coal seam is mainly mining, and the 9101 working face is the first mining face. The coal seam inclination angle is 2 – 4° and the mining height is 3.0 m. The working face is buried 200 m. The incline length of working face is 150 m, the strike length is 480 m, and the length of GERRC is 457 m. According to the lithology histogram, the direct roof is mudstone, the basic roof is sandy mudstone, and the overlying strata is the goaf of 8101 working face. The floor is fine sandstone and mudstone with large thickness. Therefore, the test roadway is a typical working face under the goaf in close-distance coal seams. The test roadway is a rectangular roadway with the height 4.0m and width 3.0m. The layout of working face is shown in Fig.1(b).

2. TECHNOLOGY OF GERRC

The technology of GERRC without coal pillar uses the BCTE technology to cut off the roof connection between roadway and stope. It can cut off the stress transfer path in the mining process and keep the roadway in a low stress area. During the process, the specific supporting technology will be used to maintain the gob-side entry stability and the gangue automatically collapses to form gangue side under the mine pressure. When the technology is applied to the working face under goaf in close-distance coal seams, the process of GERRC is shown in Fig.2.

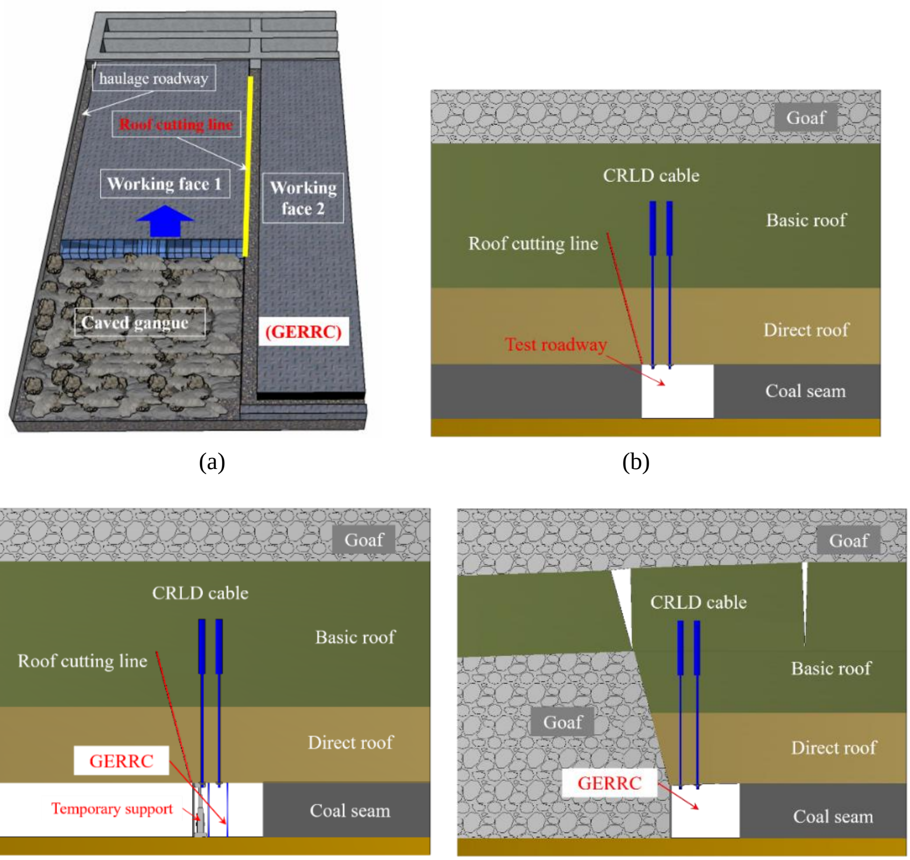

(a) (b) (c) (d)

Fig.2 Process of GERRC under goaf. (a) The principle. (b) Stage 1. (c) Stage 2. (d) Stage 3

Firstly, on the baisc roof support, the constant resistance and large deformation (CRLD) anchor cable is used to reinforce roadway roof. Secondly, The BCTE technology is carried out to form a roof cutting seam in advanced working face along the goaf side at a certain RCH and RCA, so as to cut off the roof connection and stress transfer path (Fig.2(b)). Thirdly, when the working face is mined, the roadside gangue support and the temporary support in roadway were used to maintain the roadway stability and prevent the gangue flowing into the roadway, at the same time, suppress the bending and large deformation of the roadway roof (Fig.2(c)). Fourthly, when the mine pressure and the roadway deformation are stable, the temporary support measures in the roadway will be withdrawn to achieve no-pillar mining. And the roadway will be reused for the next working face (Fig.2(d)).

4. ANALYSIS OF KEY PARAMETERS

4.1 THEORETICAL ANALYSIS

1) Roof cutting height (RCH)

The RCH refers to the maximum height of vertical upward along the roadway roof, which aims at cutting off the roof connection between stope and roadway. The gangue of stope collapses rapidly after mining, and after breaking and expanding, it can realize the supporting effect on the basic roof and reduce the rock strata movement intensity. If the RCH is small, the height of caving gangue is insufficient, the motion intensity of rock strata is severe, and the stress transfer path cannot be cut off completely. Oppositely, if the RCH is large, the speed and accumulation height of gangue collapse will increase, and it can achieve better pressure relief effect, but the difficulty and cost of BCTE will increase accordingly. Therefore, when GERRC is applied under the goaf in close-distance coal seams, the RCH should meet following principles: Firstly, after the caving gangue broking and expanding, the accumulated gangue height within the range of RCH can better realize the supporting effect on the basic roof; Secondly, the RCH should be no less than the falling zone height of stope after mining; Thirdly, on the premise of meeting the first and second principle, the RCH should be less than the distance between coal seams.

For the first principle, when the working face is mined, the stope roof collapses under pressure with broken and expansion (Fig.3). The gap between the gangue and the basic roof is (Chen et al 2019):

$$\Delta = \sum h_i + h_m - \sum K_i h_i - h_d - h_t \tag{1}$$

Where: $\sum h_i$: sum of thickness of each rock layer within RCH. h_m : the thickness of coal seam. K_i : broken expansion coefficient of each rock layer within RCH. h_d : the floor heaven. h_t : roof subsidence.

In order to reduce the amount of roof rotated subsidence and weaken the movement of rock strata, the $\Delta = 0$ need to be satisfied, then :

$$h_c = \sum h_i = \frac{h_m - h_d - h_t}{K_i - 1} \tag{2}$$

Where: h_c : the RCH.

According to the geological conditions of 9101 working face and field monitored date, the thickness of coal seam is 3.0m, the broken expansion coefficient was 1.40 and the floor heaven was 0.1m. In order to ensure the safe height, the roof subsidence was set 0.0 m. The result of RCH is 7.25m.

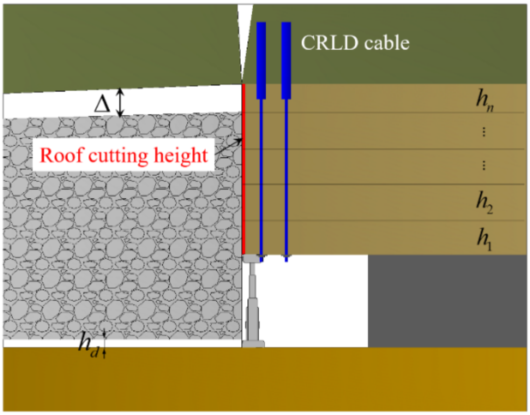

Fig.3 The calculation model of RCH

For the second principle, because the roof of 9101 working face is mudstone and sandy mudstone, and the upper coal mining caused disturbance and damage to the interlayer rock mass. Therefore, when the 9101 working face was mined, the calculation formula of the falling zone height is :

$$h_k = \frac{100h_m}{6.2h_m + 32} \pm 1.5 \tag{3}$$

Where: h_k : falling zone height.

So, the calculated falling zone height was 4.43-7.43 m. In order to realize the effect of roof cutting and pressure relief well, the RCH was 7.43m.

Based on the above analysis, the RCH should take the maximum value between h_c and h_k :

$$h_{rc} = \max\left(h_c, h_k\right) \tag{4}$$

According to Eq.(4), the reasonable RCH was7.43m. For construction convenience, the final RCH is 7.5m. The distance between NO.8 coal seam and NO.9 coal seam is 12.2 m, which was greater than the value of theoretical calculation. And it met the requirement of third principle.

2) Roof cutting angle (RCA)

The RCA refers that under the premise of determined RCH, the roof cutting seam inclines to the goaf side at a certain angle. This will make the stope roof collapse smoothly along the roof cutting seam, and not cause extrusion on the roadway roof. If the RCA is small, there will be squeeze pressure on the roadway roof in the process of gangue caving and the rotation and subsidence of the basic roof. Contrarily, if the RCA is large, the length of short-wall beam increases. It will increase the stability control and roof cutting difficulty of GERRC. Therefore, when GERRC is applied under the goaf in close-distance coal seams, the RCA should firstly satisfy the mechanical condition, that is, the rock mass damage along the predetermined structural plane. And then satisfy the geometric condition, that is, the basic roof of stope does not squeeze the roadway roof in the process of rotary subsidence.

For the mechanical condition, the roof cutting seam can be simplified as a single structural plane of rock mass. When the stope gangue collapses along the roof cutting seam under the mine pressure, it can be regarded as the shear failure of rock mass along the structural plane. The structural plane indication was shown in Fig.4(a). The theoretical analysis of rock mass failure and structural plane failure were shown in Fig.4(b).

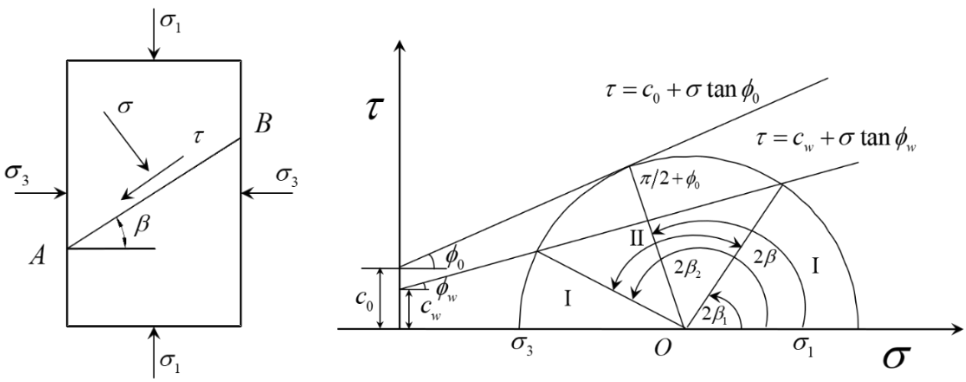

(a) (b)

Fig.4 Rock failure analysis diagram with structural plane. (a) Structure plane diagram. (b) Strength analysis diagram of rock mass with structural plane.

The normal stress and shear stress acting on the structural plane are :

$$\left.\begin{aligned} \sigma &= \frac{1}{2}(\sigma_1+\sigma_3)+\frac{1}{2}(\sigma_1-\sigma_3)\cos 2\beta \\ \tau &= \frac{1}{2}(\sigma_1-\sigma_3)\sin 2\beta \end{aligned}\right\} \tag{5}$$

Where: σ_1: maximum principal stress. σ_3: minimum principal stress. β: angle between structural plane and horizontal line.

In the process of shear failure of rock mass and structural plane, they conform to the Coulomb criterion:

$$\left.\begin{aligned} \tau &= \sigma \tan\phi_0 + c_0 \\ \tau &= \sigma \tan\phi_w + c_w \end{aligned}\right\} \tag{6}$$

Where: ϕ_0: internal friction angle of rock mass. c_0: cohesion of rock mass. ϕ_w: internal friction angle of structural plane; c_w: cohesion of structural plane.

If the rock mass is destroyed along the structural plane, it needs to change in a certain angle range. According to the relationship between rock structural plane and rock mass strength, when the angle between the structural plane and the maximum principal stress is located in region II (Fig.4(b)), the rock mass is destroyed along the structural plane, that is $\beta_1 < \beta < \beta_2$:

$$\left.\begin{aligned} \frac{\frac{\sigma_1-\sigma_3}{2}}{\sin\phi_w} &= \frac{c_w \cot\phi_w + \frac{\sigma_1+\sigma_3}{2}}{\sin(2\beta_1-\phi_w)} \\ \frac{\frac{\sigma_1-\sigma_3}{2}}{\sin\phi_w} &= \frac{c_w \cot\phi_w + \frac{\sigma_1+\sigma_3}{2}}{\sin(\pi+\phi_w-2\beta_2)} \end{aligned}\right\} \tag{7}$$

The relationship between β and RCA is $\theta = \frac{\pi}{2} - \beta$. The range of RCA is: $\theta_1 < \theta < \theta_2$

$$\left.\begin{aligned} \theta_1 &= -\frac{\phi_w}{2} + \frac{1}{2}\arcsin\left[\frac{(\sigma_1+\sigma_3+2c_w\cot\phi_w)\sin\phi_w}{\sigma_1-\sigma_3}\right] \\ \theta_2 &= \frac{\pi}{2} - \frac{\phi_w}{2} - \frac{1}{2}\arcsin\left[\frac{(\sigma_1+\sigma_3+2c_w\cot\phi_w)\sin\phi_w}{\sigma_1-\sigma_3}\right] \end{aligned}\right\} \tag{8}$$

The depth of 9101 working face is 200m, $\sigma_1 = 5MPa$,when the working face is mined, the σ_3 is regarded as 0MPa. The direct roof is mudstone, The rock test showed that: $c_0 = 1.02MPa$, $\phi_0 = 26°$.

According to Eq.(8), when the RCA is greater than 13.77°, and less than 50.23°, the shear failure will take place along the structural plane, and the stope roof will be destroyed along the roof cutting seam after mining.

For the geometric condition, in the process of caving and compaction, the basic roof of stope will gradually break. And the key Blocks A, B and C are formed near the gob-side entry (Fig.5(a)).

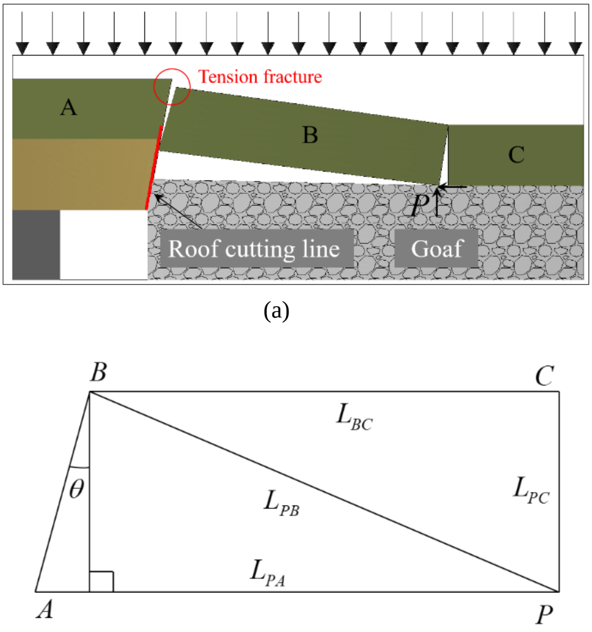

Fig.5 Geometric conditions of roof cutting angle. (a) Model of roof collapse. (b) Geometric model of Block B.

In order to reduce the extrusion friction between Block B and roadway roof, Block B should not be contact with the roadway roof when it is rotary subsidence along P point. Therefore, the geometric condition of $L_{PA} \geq L_{PB}$ should be satisfied (Fig5(b) :

$$\left.\begin{aligned} L_{PB} &= \sqrt{L_{BC}^2 + L_{PC}^2} \\ L_{PA} &= L_{BC} + L_{PC}\tan\theta \\ L_{PC} &= h_d - h_{rc} \end{aligned}\right\} \tag{9}$$

Where: L_{BC} : the length of Block B; θ : the RCA; h_d : the distance between coal seams; h_{rc} : the RCH.

From Eq.(9) :

$$\theta \geq \arctan\left(\frac{\sqrt{L_{BC}^2 + (h_d - h_{rc})^2} - L_{BC}}{h_d - h_{rc}}\right) \tag{10}$$

The length of Block B is (Li et al) :

$$L_{BC} = L\left(\sqrt{\frac{L^2}{L_w^2}+\frac{3}{2}}-\frac{L}{L_w}\right) \tag{11}$$

Where: L :the broken step of basic roof. L_w : the inclined length of working face.

According to the engineering geological conditions and monitoring data of hydraulic support with sensor: $h_d = 12.2m$, h_{rc}=7.5m , $L_w = 150m$, $L = 10m$. The range of RCA is: $\theta \geq 11°$

According to the above research, the RCA should meet the mechanical condition and the geometric condition at the same time. However, if the RCA is equal to the friction angle of rock mass, the Block B will lose stability and collapse along the roof cutting seam (Chen et al 2019). The reasonable range of RCA should be greater than 13.8° and be greater than 11°,and be less than 26°, that is : $13.8° \leq \theta < 26°$.

4.2 NUMERICAL SIMULATION ANALYSIS

According to the geological conditions of the 9101 Working face of Xiashanmao Coal Mine, the finite difference software FLAC^{3D} was used to establish a numerical simulation. The different RCH and RCA was studied. The calculation model is shown in Fig.6. The calculation range was 218 m×210 m×100 m (length×width×height). The model consists 9 layers of strata, including NO.8 coal seam and NO.9 coal seam. The model was fixed around to limit the horizontal movement, and the bottom was fixed to limit the vertical movement. The top surface was the stress boundary, and 3.30 MPa uniform load was applied to the top surface to simulate the overlying strata. The Mohr-Coulomb constitutive model was selected, and the physical and mechanical parameters of rock mass were shown in Table 1.

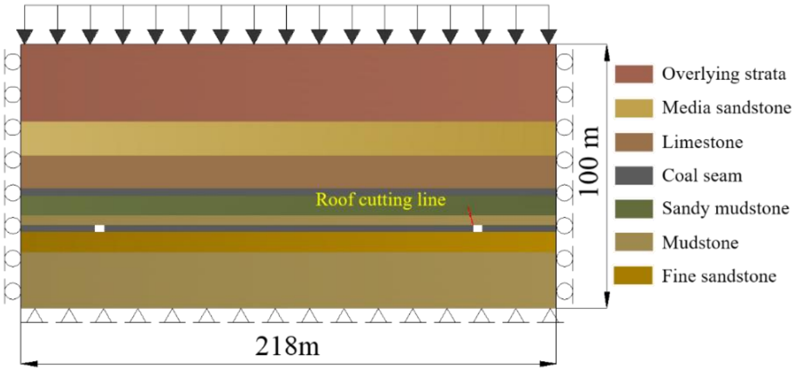

Fig.6 Schematic diagram of numerical analysis model

Table.1 The physical and mechanical parameters of rock mass

Lithology	Density, kg/m3	Bulk Modulus, GPa	Shear Modulus, GPa	Tensile Strength, MPa	Cohesion, MPa	Internal Friction Angle, °
Overlying strata	2500	3.60	2.46	1.35	1.50	28
Medium Sand-stone	2700	7.60	5.16	2.20	2.70	35
Limestone	2910	7.32	4.70	2.10	2.34	34
8 # coal seam	1450	1.91	1.15	0.35	1.35	22
Sandy mud-stone	2531	3.60	2.84	1.41	1.30	27
9 # coal seam	1450	1.91	1.15	0.35	1.35	22
Fine sandstone	2600	6.30	4.50	1.84	2.75	32
Mudstone	2460	3.10	2.17	1.60	1.02	26

According to the actual working layout conditions, the NO.8 coal seam was mined firstly step by step, and each excavation step was set as 10 m. After each step was balanced, the next step was carried out. When the NO.8 coal seam was mined out, the displacement was cleared. The mining roadway was excavated and then and 9101 working face was mined step by step. The stress distribution characteristic and deformation of surrounding rock with different RCH and RCA were studied.

1) Simulation of different RCH

In order to study effect of GERRC with different RCH, three roof cutting heights simulation schemes were proposed. The first scheme was 5.0 m, which was slightly higher than the direct roof. The second scheme was 7.5 m, which was equal to the theoretical calculation value. The third scheme was 9.0 m, which was higher than the theoretical calculation value. The RCA was set as 0°, namely, perpendicular to the roof. The results of numerical simulation were shown in Fig.7 and Fig.8.

The vertical stress distribution cloud diagrams with different RCH were shown in Fig.7. There was obvious stress concentration area on the right side of the solid coal side. When RCH was 5.0 m (Fig7(a)), 7.5 m (Fig.7(b)) and 9.0 m (Fig.7(c)), the stress concentration area of the solid coal side was respectively 3.2 m, 5.3 m and 5.5 m away from the surface of roadway surface, and the peak value of stress concentration was 21.5MPa, 20.2MPa and 19.6MPa. It indicated that with the increase of RCH, the peak value of concentration stress decreased gradually, and the stress concentration area was farther from the surface of roadway coal side. When the RCH was less than theoretical value, the stress transfer path cannot be cut off completely, the stress concentration was larger, when the RCH was greater than the theoretical calculation value, the weaken effect of pressure relief was not obvious.

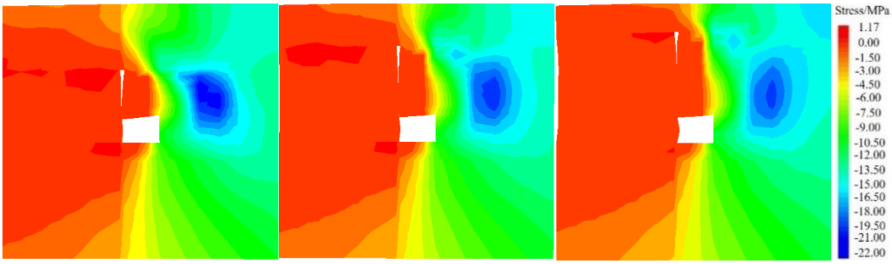

(a) (b) (c)

Fig.7 Vertical stress distribution cloud diagram of different roof cutting height. (a) Stress diagram with 5.0m.(b) Stress diagram with 7.5m. (c) Stress diagram with 9.0m.

The vertical displacement cloud diagrams with different RCH were shown in Fig.8. When RCH was 5.0m (Fig8(a)), 7.5m (Fig.8(b)) and 9.0m (Fig.8(c)), the maximum roof subsidence of roadway was respectively 440mm, 290mm and 270mm. This indicated that the roof subsidence decreased gradually with the RCH increase. When RCH was less than theoretical value, the roof subsidence was largest. When RCH was theoretical value, the roof subsidence decreased significantly. When RCH was greater than theoretical value, decrease of roof subsidence was less evident.

Through comprehensive analysis, when the RCH was equal to 7.5m, the stress transfer path can be cut off. The peak value of stress concentration and roof subsidence were relatively small, Therefore, the RCH of 9101working face under goaf should take 7.5m, that was the theoretical value.

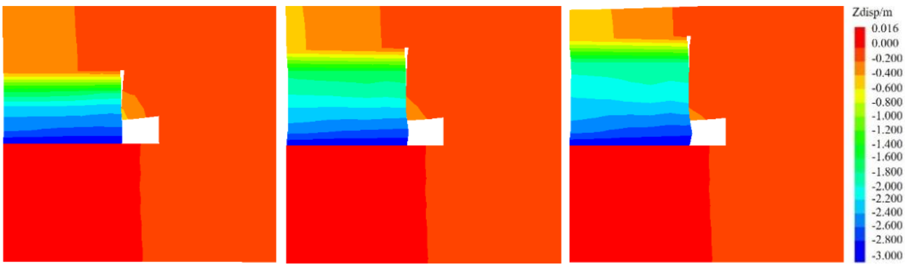

(a) (b) (c)

Fig.8 Displacement distribution cloud diagram of different roof cutting height. (a) Displacement diagram with 5.0m.(b) Displacement diagram with 7.5m. (c) Displacement diagram with 9.0m

2) Simulation of different RCA

In order to study effect of GERRC with different RCA, When RCH was 7.5m, three RCA simulation schemes were proposed. The first scheme was 10°, a little small than theoretical angle. The second and third schemes were 15° and 20°. The numerical simulation results were shown in Fig.9 and Fig.10.

The vertical stress distribution cloud diagrams with different RCA were shown in Fig.9(a)-Fig.9(c). The stress concentration area decreased. When RCA was 10° (Fig9(a)), 15° (Fig.9(b)) and 20° (Fig.9(c)), the peak value of stress concentration was respectively 20.1 MPa, 19.5 MPa and 19.5 MPa. The area and peak value of stress concentration firstly decreased and then increased.

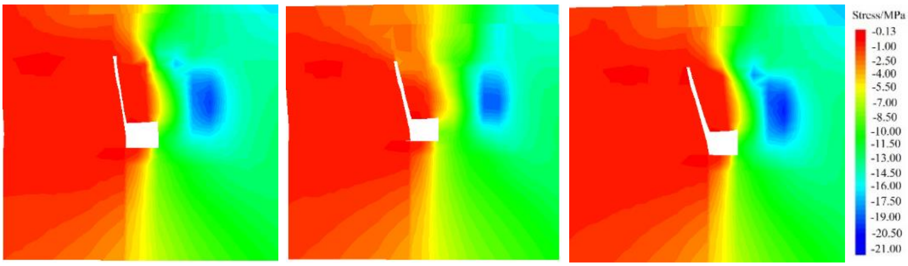

(a) (b) (c)

Fig.9 Vertical stress distribution cloud diagram with different roof cutting angle. (a) Stress diagram with 10 degrees.(b) Stress diagram with 15 degrees. (c) Stress diagram with 20 degrees.

The vertical displacement cloud diagrams with different RCA were shown in Fig.10(a)- Fig.10(c). It could be seen that roof subsidence decreased when there was a certain RCA. When RCA was 10° (Fig.10(a)), 15° (Fig.10(b)) and 20° (Fig.10(c)), the maximum roof subsidence of roadway was respectively 245mm, 196mm and 250mm. When RCA was smaller than theoretical value, the roof subsidence was larger. When RCA was in the theoretical range, the length of the roof cutting short wall beam structure increased gradually with the increasing of RCA, and the roof subsidence also increased gradually.

Through comprehensive analysis, When RCA was less than the theoretical angle, the stope roof caving still affected the roadway roof. The peak value of stress concentration and the roof subsidence of roadway were relatively larger. When RCA was within the theoretical range, with the increase of the roof cutting angle, the peak value of stress concentration and roof subsidence increased gradually. Therefore, the reasonable RCA of 9101 working face was 15°.

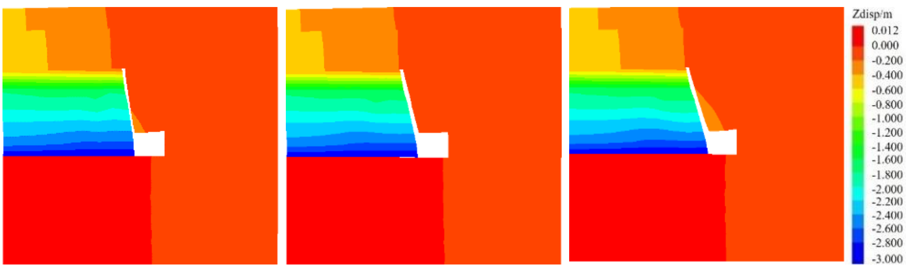

(a) (b) (c)

Fig.10 Displacement distribution cloud diagram with different roof cutting angle. (a) Displacement diagram with 10 degrees.(b) Displacement diagram with 15 degrees. (c) Displacement diagram with 20 degrees.

4.3 ANALYSIS OF CHARGE PARAMETERS

The key of GERRC is to form a roof cutting seam with a specified height and angle through BCTE technology along the goaf side of test roadway. In order to determine the pre-splitting blasting charge parameters, the control variable method was used to study the blasting charge parameters. The spacing of blasting hole was 600mm, and the length of the sealing mud was 2.0m. Four energy gathering pipes were used. Each energy gathering pipe was 1.50m. The emulsion explosive was used with the specification . Through the single-hole blasting test, the reasonable charge range was 11-12 rolls in each blasting hole. On this basis, the optimal charge parameters are studied by the continuous hole blasting test. The blasting scheme and the energy gathering pipe were shown in Fig.11(a) and Fig.11(b). The fracture penetration rate and fracture characteristics of different charge parameters were shown in Table 2.

Table 2. On-site test parameter table of shaped charge blasting

Test scheme	Charge parameter /roll	Fracture penetration rate	Fracture characteristics
1	3+3+2+1	54.3%	Crack spacing occurred and low fracture penetration rate
2	4+4+3+1	72%	Cracks continuously occurred in the middle and upper part, but not occurred in the lower part
3	4+3+3+2	91%	Crack penetration effect was good, met the design requirements

By comparing the fracture penetration rate and fracture characteristics of different charge parameters, the optimal charge parameter was 4+3+3+2, the seam rate was 111 %, and the crack penetration effect was better. This could meet the requirements of GERRC and ensure the effect of roof cutting and pressure relief. The charge parameter structure and the effect of BCTE were shown in Fig.11 (c) and Fig.11 (d).

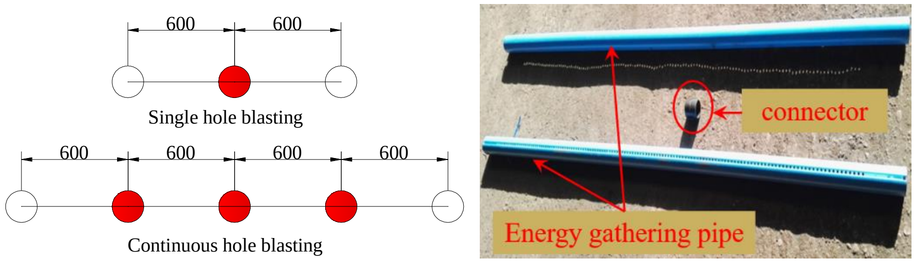

（a） （b）

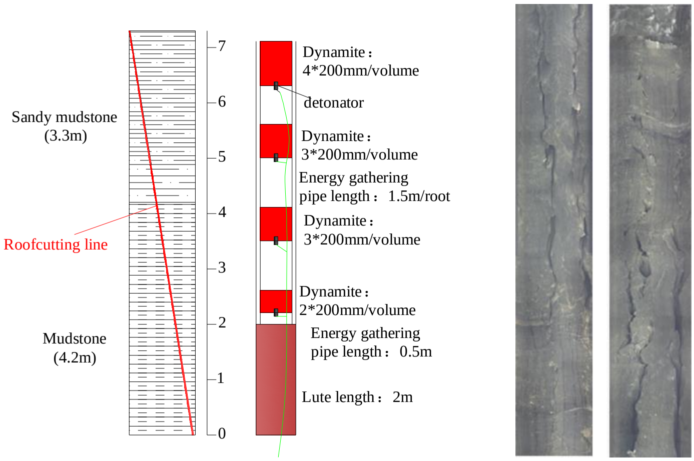

（c） (d)

Fig.11 Blasting test schematic and crack effect diagram. (a) Single hole and continuous hole blasting schematic diagram. (b) Schematic diagram of energy gathering pipe. (c) Schematic diagram of chart. (d) Effect of BCTE

5. ENGINEERING APPLICATION AND EFFECT

5.1 SUPPORT DESIGN

The support design of GERRC was divided into two steps, they were reinforcement support and temporary support.

The first step was reinforcement support. Three rows of constant resistance and large deformation (CRLD) anchor cables were used to reinforce the roadway roof of 9101 working face. The diameter of CRLD was 21.8 mm and the length was 9300 mm. The constant resistance value was 32 ± 3 t. The length of the constant resistance device was 460 ± 5mm. The pre-tightening force was set as not less than 25 t. The first row spacing of CRLD cables was 1.0 m, and the W steel strip was used to connect two cables. The second row spacing of CRLD cables was 2.0m. The steel ladder beam was used to connect two cables. The third row spacing of CRLD cables was 5.0m. It was applied in the form of point anchorage and tilted 15° to solid coal side. The sectional view and plan view diagram were shown in Fig.12(a) and Fig.12(b).

The second step was temporary support. Before mining, in order to reduce the influence of advanced mining stress, three single hydraulic props and a π-beam were used at 20 m ahead of working face (Fig.12(a)). After mining, in order to reduce the deformation of roadway surrounding rock, one unit support, two single hydraulic props and one π-shaped beam were combined for temporary support in roadway (Fig.12(c)), and the spacing of single hydraulic props was 1200 mm. Meanwhile, the U-shaped shrinkable steel and diamond metal mesh were introduced as side support to prevent the caving gangue from pouring into the roadway, the spacing of U--shaped shrinkable steel was shown in Fig.12(d).

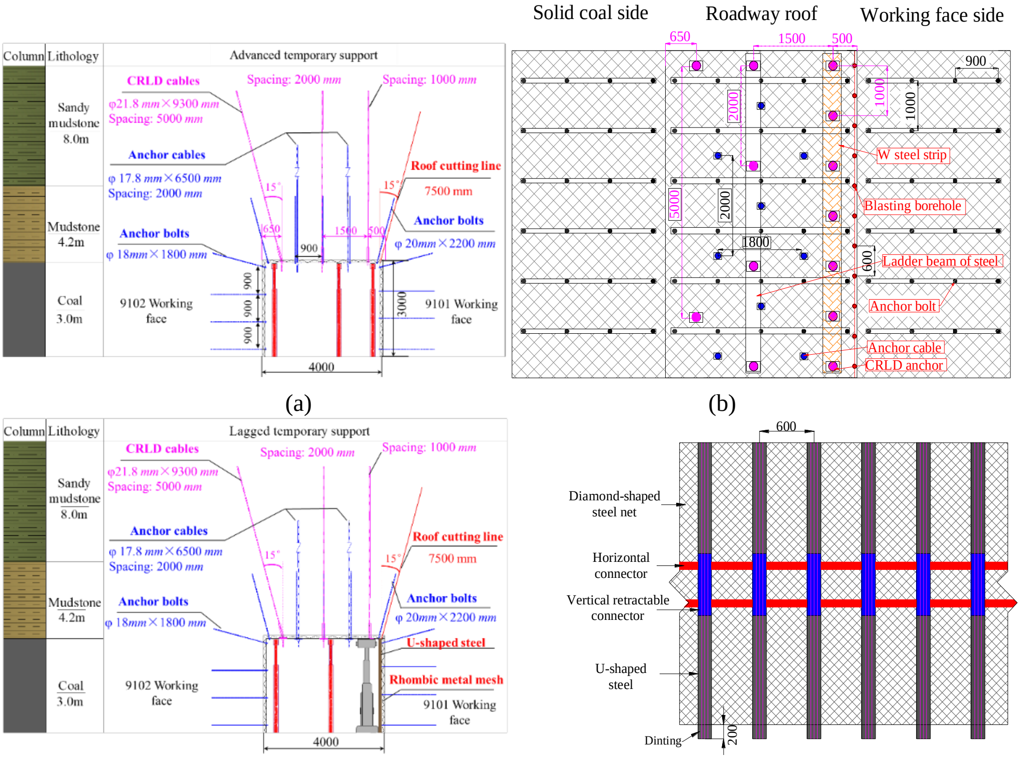

Fig.12 Support design diagram. (a) Sectional view of support design in advance of working face. (b) Plane view with CRLD anchor cable. (c) Sectional view of support design lagged working face. (d) Section view of roadside gangue support.

The deformation of the surrounding rock can effectively reflect the effect of GERRC. After the 9101 working face was mined, the deformation of surrounding rock of the test roadway was monitored by cross measuring point method. The roof subsidence, deformation of goaf side and solid coal side, the floor heaven were monitored. In order to ensure the effectiveness of deformation monitoring, the monitoring data of two stations were selected for analysis. The surrounding rock deformation curve of different stations lag working face in RFARC was shown in Fig.13.

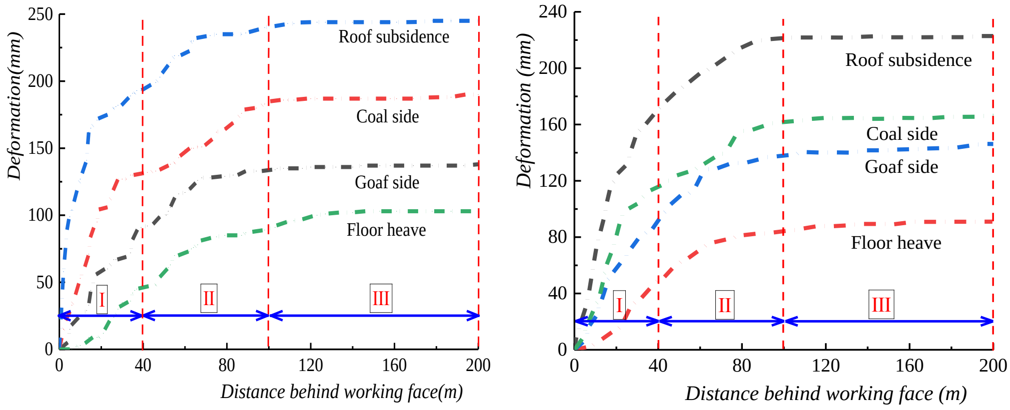

(a) (b)

Fig.13 Deformation curve of surrounding rock. (a) Station 1. (b) Station 2.

According to the deformation curve of surrounding rock (Fig.13), when the working face was mined, the deformation of surrounding rock had obvious zoning characteristics. When lagged behind 0-40m, the deformation increasing rate of surrounding rock was large. It was the rapid deformation zone. When lagged behind 40-100m, the deformation increasing rate of surrounding rock decreased. It was the deceleration deformation zone. When lagged behind more than 100m, the deformation of surrounding rock tended to be stable. It was the stable deformation zone. The maximum deformation of roof was between 240mm to 250mm. The maximum deformation of coal side was between 160mm to 170mm. The maximum deformation of goaf side was nearly 125mm, and floor heaven was nearly 80mm to 100mm.

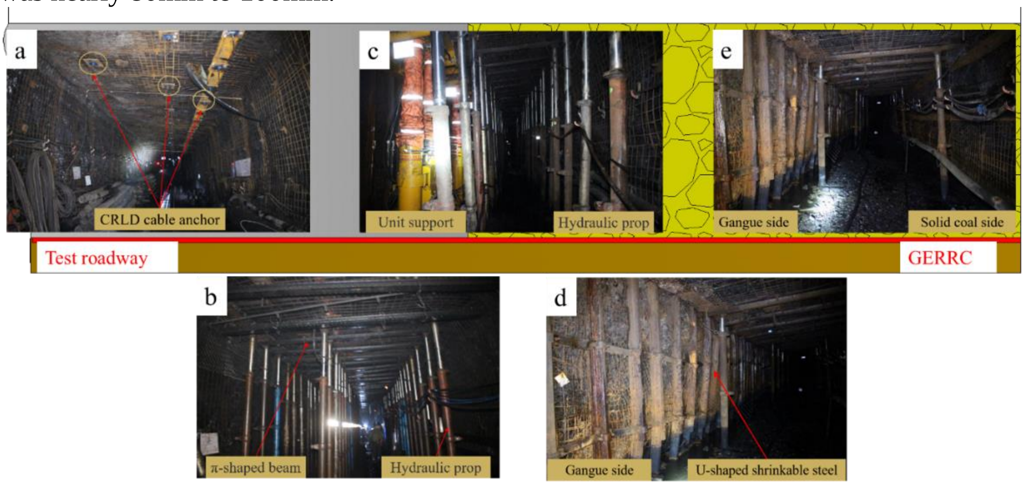

Fig.14 Effect of on-site support and effect of GERRC when the temporary support was withdrawn.(a) Support with CRLD anchor cables (b)Temporary support effect of advanced working face (c) Temporary support effect when lagged working face (c) Effect of Goaf side. (d) Overall effect of GERRC.

When lagged behind working face 120m, the movement of roof strata and the deformation of surrounding rock of GERRC were stable, then the temporary support in roadway was withdrawn. The effect diagram of temporary support on site and the withdrawal of temporary support were shown in Fig.14. It can be seen that U-shaped shrinkable steel and connectors were well to prevent the collapse of gangue into the roadway. The overall effect of GERRC was good under the design of strength support to roof and coal side and temporary support in roadway.

6. CONCLUSION

When GERRC was applied in working face under goaf of close-distance coal seams, the RCH should satisfy the supporting effect of gangue on the basic roof after broken and expansion, and should be greater than the caving height of stope roof, meanwhile, it should be less than the coal seams spacing. The RCA should meet the mechanical condition and geometric condition at the same time.

Combining theoretical analysis and numerical simulation, when the RCH was 7.5 m and the RCA was 15°, the stress field and roof subsidence of GERRC were optimal. It not only cut off the stress transfer path between the stope roof and roadway roof, but also reduced the influence of rotary subsidence of the basic roof on the roadway roof.

The charge parameters of BCTE were tested by control variable method. When the blasting hole spacing was 600 mm and the length of sealing mud was 2.0 m, the optimal charge structure parameters were 4+3+3+2, and the crack rate reached 91%.

When the roadway roof was reinforced by three columns of CRLD anchor cable and the temporary support was consisted with unit support and single hydraulic prop could effectively control the deformation of surrounding rock, and when lagged behind working face 120 m, the deformation of surrounding rock tended to be stable.

ACKNOWLEDGEMENTS

This work was supported by Open Fund of State Key Laboratory of Coal Resources and Safe Mining (Grant No.SKLCRSM20KFA11); the State Key Laboratory for Geomechanics and Deep Underground Engineering, China University of Mining & Technology, Beijing (SKLGDUEK2017); the Fundamental Research Funds for the Central Universities (Grant No. 2022YJSLJ09).

REFERENCE

Chen SY, Zhao F, Wang HJ, Yuan GX, Guo ZB, Yang J (2019) Determination of key parameters of gob-side entry retaining by cutting roof and its application to a deep mine. Rock and Soil Mechanics. 40(1): 332-350. 10.16285/j.rsm.2017.2194.

Cheng Zhiheng, Qi Qingxin, Kong Weiyi, Zhang lang, Ji Wenbo, Liu Xiaogang (2015) Study on the reasonable layout of gob-side remained gateway of lower coal seam close to coal seam group. Journal of Mining & Safety Engineering. 32(03):453-458.

Gao X., Zhang S., Zi Y., Pathan Sakib-khan (2020) Study on optimum layout of roadway in close coal seam. Arab J Geosci 13, 746. https://doi.org/10.1007/s12517-020-05722-y.

Hao DY, Wu YZ, Chen HJ, Chu XW, Li Y. (2019) Instability mechanism and prevention technology of roadway in close distance and extra thick coal seam under goaf. Journal of China Coal Society 44(9) : 2682－2690. 10.13225/j.cnki.jccs.2019.0217.

He MC, Cao WF, Shan RL, Wang SL (2003) New blasting technology——bilateral cumulative tensile explosion. Chinese Journal of Rock Mechanics and Engineering 22(12): 2047-2051. CNKI:SUN:YSLX.0.2003-12-019.

He MC, Ma ZM, Guo ZB, Chen SY (2018) Key parameters of the gob-side entry retaining formed by roof cutting and pressure release in deep medium-thickness coal seams. Journal of China university of mining and technology 47(3): 468-477. 10.13247/j.cnki.jcumt.000852.

He MC, Zhu GL, Guo ZB (2015) Longwall mining “cutting cantilever beam theory” and 110 mining method in China——The third mining science innovation. Journal of Rock Mechanics and Geotechnical Engineering,7(05):483-492. https://doi.org/10.1016/j.jrmge.2015.07.002.

Hu JZ, He MC, Wang J, Ma ZM, Wang YJ, Zhang XY (2019) Key parameters of roof cutting of gob-side entry retaining in a deep inclined thick coal seam with hard roof. Energies 12: 934. https://doi.org/10.3390/en12050934 .

Ji HG, Xiang P, Zhang L, Han F, Yang ZJ (2011) Experimental study and detection analysis of mechanical properties variability of rock mass in excavation disturbance. Chinese Journal of Rock Mechanics and Engineering 30(11): 2352-2359. SUN:YSLX.0.2011-11-023.

Li YF, Hua XZ, Cai RC (2012) Mechanics analysis on the stability of key block in the gob-side entry retaining and engineering application. Journal of Mining & Safety Engineering 29(3): 357-364. CNKI:SUN:KSYL.0.2012-03-012.

Liu HQ, Wang L, Han CL, Liu P, Zou P (2021) Study on the instability mechanism and control measures of a roadway in a mine with retained coal pillars and close coal seams. Shock and Vibration. 2021,1-14. https://doi.org/10.1155/2021/8871807.

Shi LQ, Xu DJ, Qiu M, Jing X, Sun HH (2013) Improved on the formula about the depth of damaged floor in working area. Journal of China Coal Society 38 (S2):299-303. 10.13225/j.cnki.jccs.2013.s2.029.

Sun XM, Liu X, Liang GF, Wang D, Jiang YL (2014) Key parameters of gob-side entry retaining formed by roof cut and pressure releasing in thin coal seams. Chinese Journal of Rock Mechanics and Engineering 33(7): 1449-1456. 10.13722/j.cnki.jrme.2014.07.017.

Sun XM, Wang D, Yu SB, Wang C, Zheng YL, Ren XD (2014) Research on the evolutional course of surrounding rock structure along gob side with excavation of multiple working faces in close distance seam. Journal of Mining & Safety Engineering. 31(04):607-611. 10.13545/j.issn1673-3363.2014.04.018.

Teng JW, Qian YH, Song PH (2016) Analysis of exploration, potential reserves and high efficient utilization of coal in China. Chinese J. Geophys. 59(12): 4633-4653. 10.6038/cjg20161224.

Wang H.W., Jiang YD, Zhao YX, Wang T., Yang T, Ning TH (2015) Determination of reasonable roadway position during extraction of closed coal seam based on energy theory. Chinese Journal of Rock Mechanics and Engineering 34(305) (S2):4023-4029. 10.13722/j.cnki.jrme.2015.0862.

Wang LF, Chang ZC, Yang ZB, Wang XF, Qin DD (2018) Combined support technology of roadway under mined gob of ultra-distance seams in deep mine. Journal of Mining & Safety Engineering 35(4): 686-692. 10.13545/j.cnki.jmse.2018.04.004.

Wang Q, He MC, Yang J, Gao HK, Jiang B, Yu HC, 2018. Study of a no-pillar mining technique with automatically formed gob-side entry retaining for longwall mining in coal mines. Int J Rock Mech Min

Sci. 110: 1–8. https://doi.org/10.1016/j.ijrmms.2018.07.005.

Xiaoming Sun, Chengwei Zhao, Gan Li, Bo Zhang, Junwei Wang, Feng Cai (2020) Physical model experiment and numerical analysis on innovative gob-side entry retaining with thick and hard roofs. Arabian Journal of Geosciences (2020) 13: 1245. https://doi.org/10.1007/s12517-020-06238-1

Xiaoming Sun, Chengwei Zhao, Gan Li, Bo Zhang, Junwei Wang, Feng Cai (2020) Physical model experiment and numerical analysis on innovative gob-side entry retaining with thick and hard roofs. Arabian Journal of Geosciences (2020) 13: 1245. https://doi.org/10.1007/s12517-020-06238-1

Xingyu Zhang, Ronald Y.S. Pak, Yubing Gao, Chenkang Liu, Cheng Zhang, Jun Yang, Manchao He (2020) Field experiment on directional roof presplitting for pressure relief of retained roadways, International Journal of Rock Mechanics and Mining Sciences,134: 104436. https://doi.org/10.1016/j.ijrmms.2020.104436

Yan H., Weng MY, Feng RM, Li WK (2015) Layout and support design of a coal roadway in ultra-close multiple-seams. Journal of Central South University 22(11): 4385-4395. https://doi.org/10.1007/s11771-015-2987-7.

Zhang GF, He MC, Yu XP, Huang ZG (2011) Research on the technique of no-pillar mining with gob-side entry formed by advanced roof caving in the protective seam in Baijiao coal mine. Journal of Mining & Safety Engineering 28(4):511-516. CNKI:SUN:KSYL.0.2011-04-004.

Zhang XY, He MC, Yang J, Wang EY, Zhang JB, Sun Y (2020) An Innovative Non-Pillar Coal-Mining Technology with Automatically Formed Entry: A Case Study. Engineering 6(11):1315-1329. https://doi.org/10.1016/j.eng.2020.01.014.

Zhibiao Guo, Qiong Wang, Zhaohua Li, Manchao He, Zhibo Ma, Feixiang Zhong, Jie Hu (2019) Surrounding rock control of an innovative gob-side entry retaining with energy-absorbing supporting in deep mining. International Journal of Low-Carbon Technologies, 14(1): 23–35. https://doi.org/10.1093/ijlct/cty054